Probing Parity Violation with Weak Lensing Trispectrum

Sijin Chen

Universitäts-Sternwarte München
with Zhengyangguang (Laurence) Gong and Jiamin Hou

Munich LSS Day, Oct 21, 2025

Motivation

- Parity violation in cosmology —— potential signature of new physics in large-scale structure
- CMB lensing has been proposed to probe parity violation in the early universe
- Weak lensing traces matter distribution at late times, complementary to CMB

Introduction of parity

Parity transformation:

$$\mathbb{P}:\boldsymbol{x}\rightarrow-\boldsymbol{x}$$

$$\mathbb{P}:(x,y,z)\rightarrow(-x,-y,-z)$$

2PCF

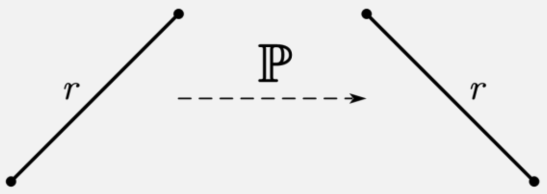

3PCF

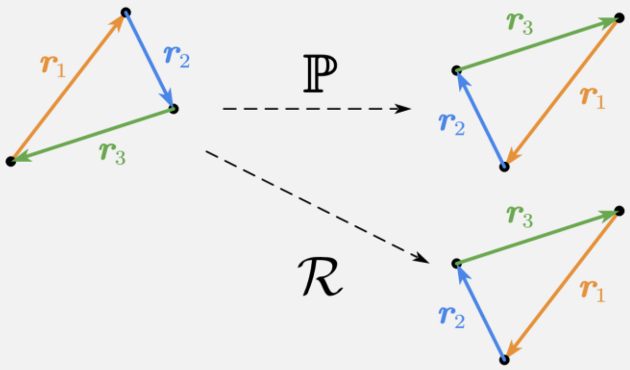

4PCF

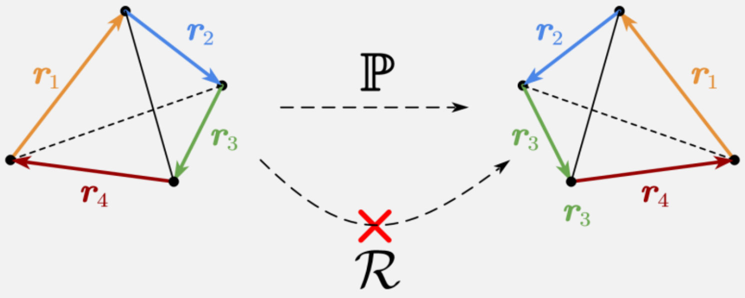

Why 2D surface doable?

- On 2D flat plane, a parity transformation is equivalent to a $180°$ rotation about the axis perpendicular to the plane through the origin.

$$\mathcal{R}(\theta) = \begin{pmatrix} \cos\theta & -\sin\theta \\ \sin\theta & \cos\theta \end{pmatrix}$$

$$\mathcal{R}(\pi) = \begin{pmatrix} \cos\pi & -\sin\pi \\ \sin\pi & \cos\pi \end{pmatrix} = \begin{pmatrix} -1 & 0 \\ 0 & -1 \end{pmatrix} = \mathbb{P} = \begin{pmatrix} -1 & 0 \\ 0 & -1 \end{pmatrix}$$

- But this is not true for 2D curved surface.

Why 2D surface doable?

- **Rotation on 2D spherical surface**

$$\mathcal{R}(\alpha,\beta,\gamma)=\mathcal{R}_x(\gamma)\mathcal{R}_y(\beta)\mathcal{R}_z(\alpha)$$
$$=\begin{pmatrix}\cos\gamma & -\sin\gamma & 0\\ \sin\gamma & \cos\gamma & 0\\ 0 & 0 & 1\end{pmatrix}\begin{pmatrix}\cos\beta & 0 & \sin\beta\\ 0 & 1 & 0\\ -\sin\beta & 0 & \cos\beta\end{pmatrix}\begin{pmatrix}1 & 0 & 0\\ 0 & \cos\alpha & -\sin\alpha\\ 0 & \sin\alpha & \cos\alpha\end{pmatrix}$$

- **Determinant:**

$$|\mathcal{R}(\alpha,\beta,\gamma)|=|\mathcal{R}_x(\gamma)|\,|\mathcal{R}_y(\beta)|\,|\mathcal{R}_z(\alpha)|=1$$

- **Parity transformation**

$$\mathbb{P}=\begin{pmatrix}-1 & 0 & 0\\ 0 & -1 & 0\\ 0 & 0 & -1\end{pmatrix}$$

- **Determinant:**

$$|\mathbb{P}|=-1$$

Greco et al. 2025

Weak lensing basics

- **Convergence, κ, is the projected matter density contrast along the line of sight**

$$\kappa(\hat{\boldsymbol{n}}) = \int_0^{\chi_H} \mathrm{d}\chi q(\chi)\delta(\chi\hat{\boldsymbol{n}}, \chi)$$

- **Lensing kernel $q(\chi)$ with Dirac delta redshift distribution:**

$$q(\chi) = \frac{3H_0^2\Omega_m}{2c^2}\frac{1}{a(\chi)}\frac{\chi(\chi_s - \chi)}{\chi_s}$$

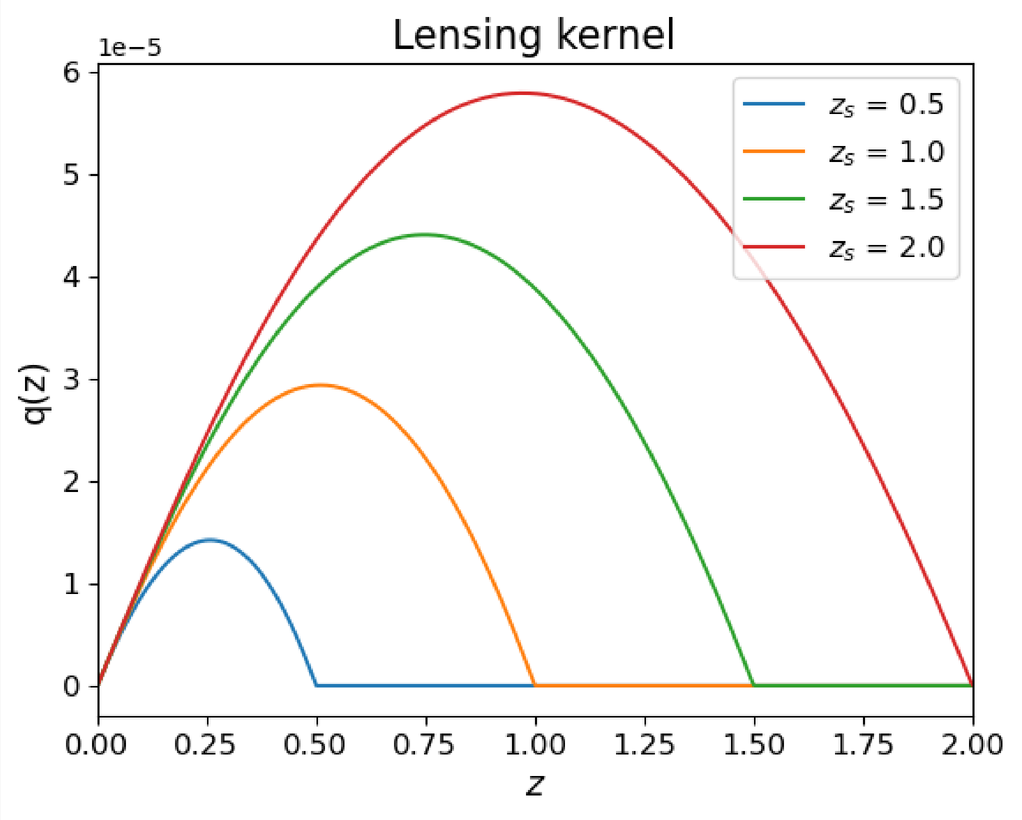

Weak lensing trispectrum

Weak lensing convergence:

$$\kappa_{\ell m} = 4\pi i^{\ell} \int_0^{\chi_H} \mathrm{d}\chi' q(\chi') \int \frac{\mathrm{d}^3 k}{(2\pi)^3} \, \tilde{\delta}(\boldsymbol{k}) j_\ell(k\chi') Y^*_{\ell m}(\hat{k})$$

Plane-wave expansion:

$$e^{i\boldsymbol{k}\cdot\boldsymbol{x}} = 4\pi \sum_{L=0}^{\infty} \sum_{M=-L}^{L} i^L j_L(kx) Y_{LM}(\hat{\boldsymbol{k}}) Y^*_{LM}(\hat{\boldsymbol{x}})$$

Angular trispectrum:

$$\langle \kappa_{\ell_1 m_1} \kappa_{\ell_2 m_2} \kappa_{\ell_3 m_3} \kappa_{\ell_4 m_4} \rangle = (2\pi)^3 (4\pi)^4 i^{\ell_1+\ell_2+\ell_3+\ell_4} \int_0^{\chi_{H_1}} \mathrm{d}\chi'_1 \ldots \int_0^{\chi_{H_4}} \mathrm{d}\chi'_4 \, q(\chi'_1) \ldots q(\chi'_4)$$
$$\times \int \frac{\mathrm{d}^3 k_1}{(2\pi)^3} \cdots \int \frac{\mathrm{d}^3 k_4}{(2\pi)^3} \, \delta_D^{(3)}(\boldsymbol{k}_1 + \boldsymbol{k}_2 + \boldsymbol{k}_3 + \boldsymbol{k}_4) T(\boldsymbol{k}_1, \boldsymbol{k}_2, \boldsymbol{k}_3, \boldsymbol{k}_4)$$
$$\times j_{\ell_1}(k_1 \chi'_1) \, j_{\ell_2}(k_2 \chi'_2) \, j_{\ell_3}(k_3 \chi'_3) \, j_{\ell_4}(k_4 \chi'_4)$$
$$\times Y^*_{\ell_1 m_1}(\hat{k}_1) \, Y^*_{\ell_2 m_2}(\hat{k}_2) \, Y^*_{\ell_3 m_3}(\hat{k}_3) \, Y^*_{\ell_4 m_4}(\hat{k}_4)$$

Weak lensing reduced trispectrum

Formula of weak lensing angular reduced trispectrum:

$$Q^{\ell_1\ell_2}_{\ell_3\ell_4}(L)=(2L+1)\sum_{m_1m_2m_3m_4M}(-1)^M\begin{pmatrix}\ell_1&\ell_2&L\\m_1&m_2&M\end{pmatrix}\begin{pmatrix}\ell_3&\ell_4&L\\m_3&m_4&-M\end{pmatrix}\langle\kappa_{\ell_1m_1}\kappa_{\ell_2m_2}\kappa_{\ell_3m_3}\kappa_{\ell_4m_4}\rangle$$

$$=(2L+1)\times i^{\ell_1+\ell_2+\ell_3}$$

$$\times\sum_{L_1L_2L_3}\sum_{L'}\mathcal{F}_{L_1L_2L'}\mathcal{F}_{L_3\ell_4L'}\times i^{L_1+L_2+L_3}\sum_{\ell_1'\ell_2'\ell_3'}\times\mathcal{F}_{L_1\ell_1'\ell_1}\mathcal{F}_{L_2\ell_2'\ell_2}\mathcal{F}_{L_3\ell_3'\ell_3}$$

$$\times(-1)^{\ell_1'+\ell_2'}\begin{Bmatrix}\ell_3&\ell_4&L\\L'&\ell_3'&L_3\end{Bmatrix}\begin{Bmatrix}L&L'&\ell_3'\\\ell_2&L_2&\ell_2'\\\ell_1&L_1&\ell_1'\end{Bmatrix}$$

Geometry part (coupling of angular modes)

$$\times\left[\frac{2}{5}\frac{1}{\Omega_{m,0}H_0^2}\right]^4\int_0^\infty\frac{d\chi}{\chi^{14}}\prod_{n=1}^{4}\left[q_n(\chi)D(\chi)\mathcal{T}_\delta\left(\frac{\ell_n}{\chi}\right)\ell_n^2\right]T^{\mathcal{R}}_{\ell_1'\ell_2'\ell_3'}\left(\frac{\ell_1}{\chi},\frac{\ell_2}{\chi},\frac{\ell_3}{\chi},\frac{\ell_4}{\chi}\right)$$

Projection part (from 3D to 2D)

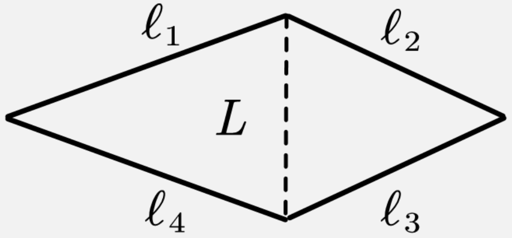

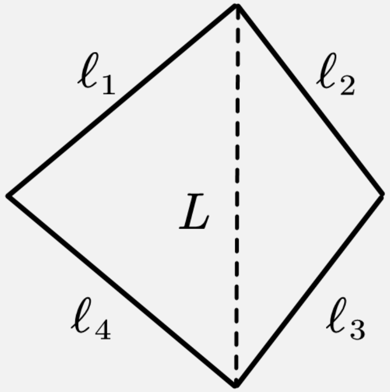

where $\mathcal{F}$ is: explain the projection, geometry and finally the total reduced trispectrum.

$$\mathcal{F}_{\ell_1\ell_2\ell_3}=\sqrt{\frac{(2\ell_1+1)(2\ell_2+1)(2\ell_3+1)}{4\pi}}\begin{pmatrix}\ell_1&\ell_2&\ell_3\\0&0&0\end{pmatrix}$$

Weak lensing trispectrum projection part

Projection part:

$$\mathcal{I}^{\ell_1'\ell_2'\ell_3'}_{\ell_1\ell_2\ell_3\ell_4}=\left[\frac{2}{5}\frac{1}{\Omega_{m,0}H_0^2}\right]^4\int_0^\infty \frac{\mathrm{d}\chi}{\chi^{14}}\prod_{n=1}^{4}\left[q_n(\chi)D(\chi)\mathcal{T}_\delta\left(\frac{\ell_n}{\chi}\right)\ell_n^2\right]T^{\mathcal{R}}_{\ell_1'\ell_2'\ell_3'}\left(\frac{\ell_1}{\chi},\frac{\ell_2}{\chi},\frac{\ell_3}{\chi},\frac{\ell_4}{\chi}\right)$$

- $D(\chi)$: linear growth factor
- $\mathcal{T}_\delta\left(\frac{\ell_n}{\chi}\right)$: linear transfer function

Primordial curvature trispectrum template:

$$T^{\mathcal{R}}_{-}(\boldsymbol{k}_1,\boldsymbol{k}_2,\boldsymbol{k}_3,\boldsymbol{k}_4)\equiv[\boldsymbol{k}_1\cdot(\boldsymbol{k}_2\times\boldsymbol{k}_3)]\,g_-\,[2\pi^2A_s]^3\left(\frac{k_1^{-2}k_2^{-1}k_3^0k_4^0}{k_1^3k_2^3k_3^3k_4^0}\mp\ 23\,\mathrm{perm.}\right)$$

- keep indices position fixed
- odd permutation → −
- even permutation → +

Coulton et al. 2024

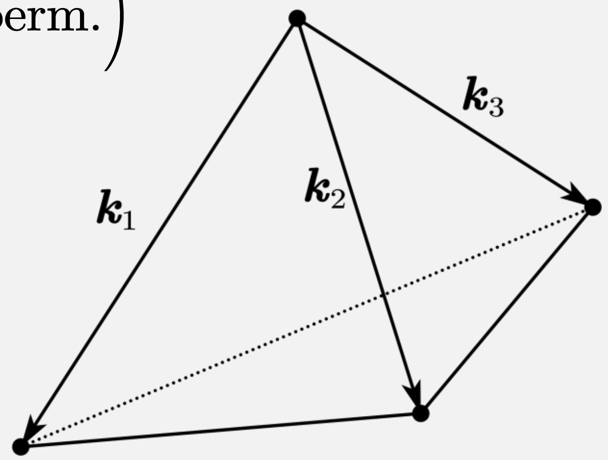

Weak lensing trispectrum projection part

- **Projection part:**

$$\mathcal{I}^{\ell_1'\ell_2'\ell_3'}_{\ell_1\ell_2\ell_3\ell_4} = \left[\frac{2}{5}\frac{1}{\Omega_{m,0}H_0^2}\right]^4 \int_0^\infty \frac{\mathrm{d}\chi}{\chi^{14}} \times \prod_{n=1}^{4} \left[q_n(\chi)D(\chi)\mathcal{T}_\delta\left(\frac{\ell_n}{\chi}\right)\ell_n^2\right] \times T^{\mathcal{R}}_{\ell_1'\ell_2'\ell_3'}\left(\frac{\ell_1}{\chi},\frac{\ell_2}{\chi},\frac{\ell_3}{\chi},\frac{\ell_4}{\chi}\right)$$

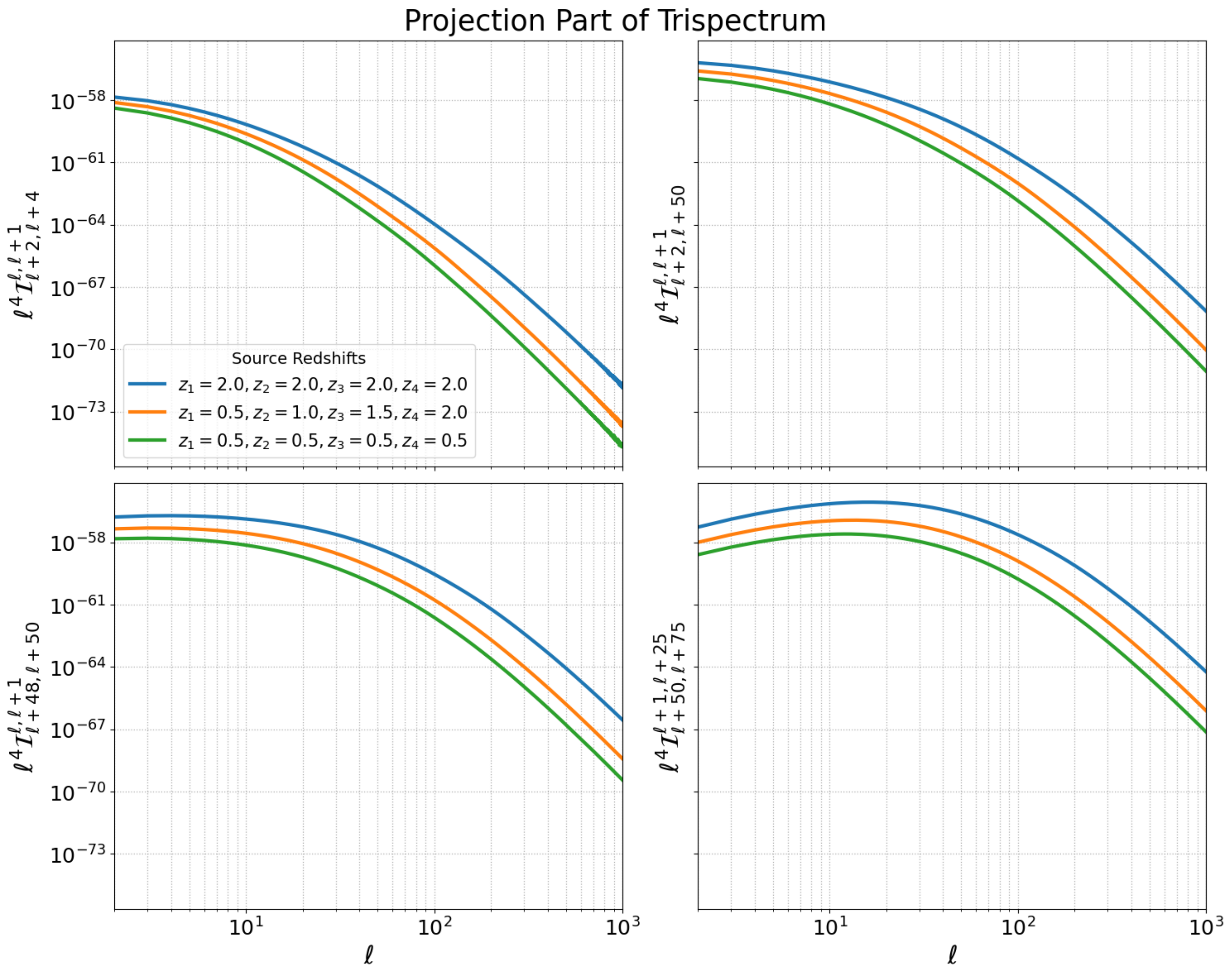

Weak lensing trispectrum geometry part

- **Geometry part:**

$$\mathcal{G} = (2L+1) \times i^{\ell_1+\ell_2+\ell_3} \times \sum_{L_1L_2L_3} \sum_{L'} \mathcal{F}_{L_1L_2L'}\mathcal{F}_{L_3\ell_4L'} \times i^{L_1+L_2+L_3} \times \sum_{\ell_1'\ell_2'\ell_3'} \mathcal{F}_{L_1\ell_1'\ell_1}\mathcal{F}_{L_2\ell_2'\ell_2}\mathcal{F}_{L_3\ell_3'\ell_3} \times (-1)^{\ell_1'+\ell_2'} \begin{Bmatrix} \ell_3 & \ell_4 & L \\ L' & \ell_3' & L_3 \end{Bmatrix} \begin{Bmatrix} L & L' & \ell_3' \\ \ell_2 & L_2 & \ell_2' \\ \ell_1 & L_1 & \ell_1' \end{Bmatrix}$$

- A fix ordering $\ell_1 < \ell_2 < \ell_3 < \ell_4$
- For each set, vary L from minimum to maximum to generate configurations
- Figure shows the reduced trispectrum for each configuration

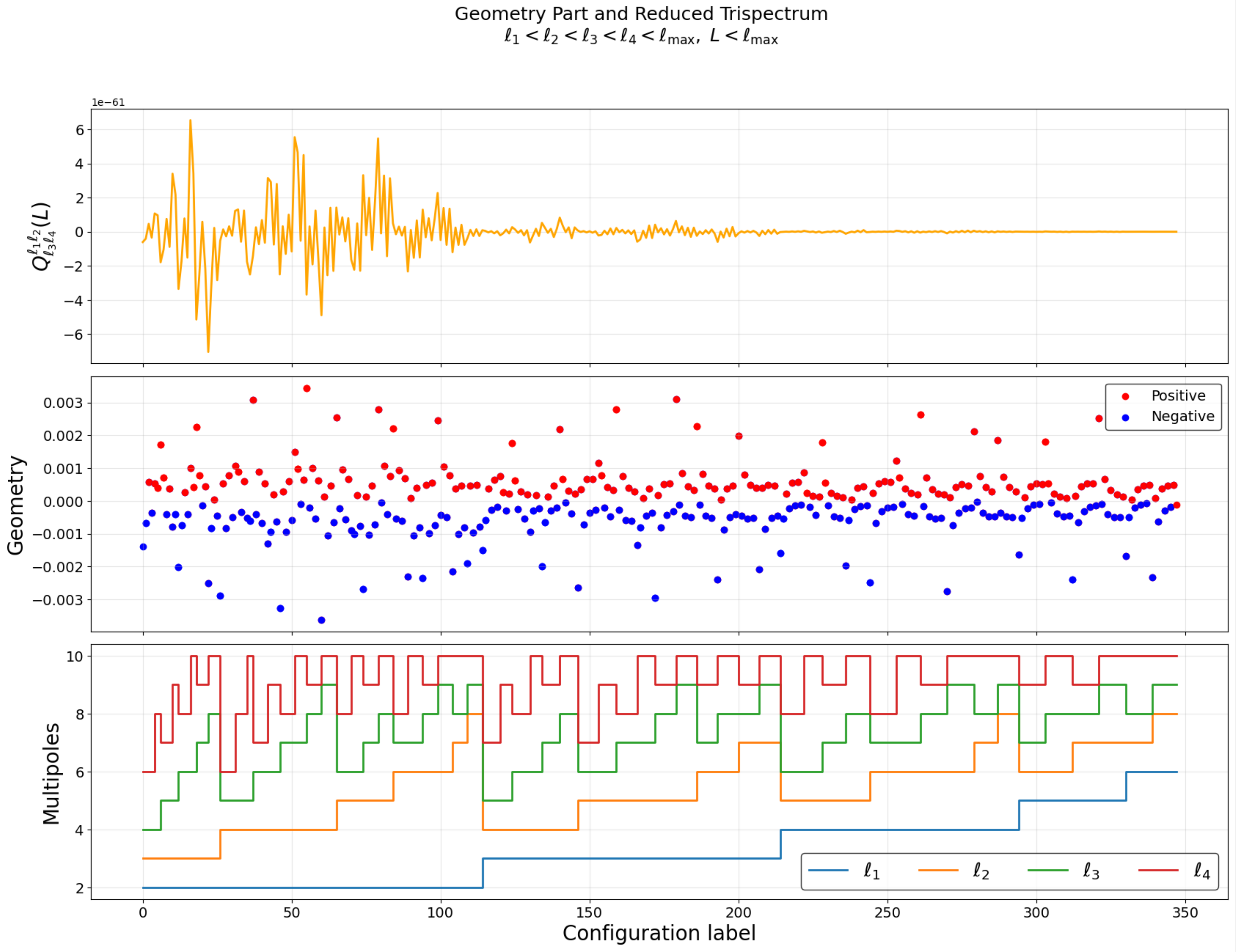

Signal-to-Noise Ratio

$$\mathrm{SNR} \approx \sqrt{\sum_{L=2}^{\ell_{\max}} (2L+1)^{-1} \sum_{\ell_1<\ell_2<\ell_3<\ell_4}^{\ell_{\max}} \frac{|Q^{\ell_1\ell_2}_{\ell_3\ell_4}(L)|^2}{C_{\ell_1}C_{\ell_2}C_{\ell_3}C_{\ell_4}}}$$

- **SNR computed with multipole summation cut as ℓ_{max}**
- **ℓ_{max} is the maximum of different combinations of $\{\ell_1, \ell_2, \ell_3, \ell_4, L\}$.**

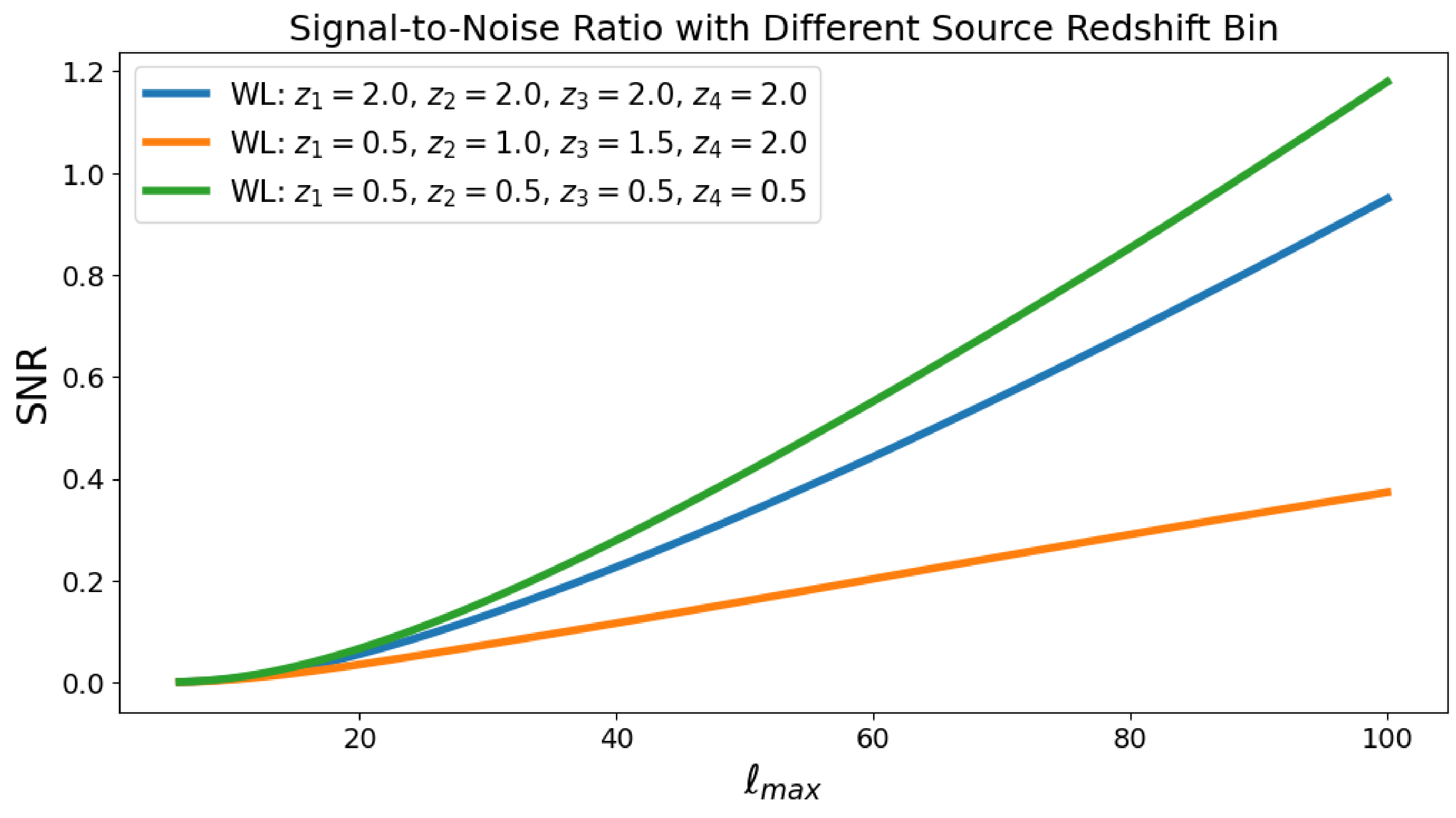

Squeezed Limit

$$\mathrm{SNR} \approx \sqrt{\sum_{L=2}^{\ell_{\max}} (2L+1)^{-1} \sum_{\ell_1<\ell_2<\ell_3<\ell_4}^{\ell_{\max}} \frac{\left|Q^{\ell_1\ell_2}_{\ell_3\ell_4}(L)\right|^2}{C_{\ell_1}C_{\ell_2}C_{\ell_3}C_{\ell_4}}}$$

- **Keep ℓ_{max} fixed and change ℓ_1**
- **Sensitive to squeezed limit**

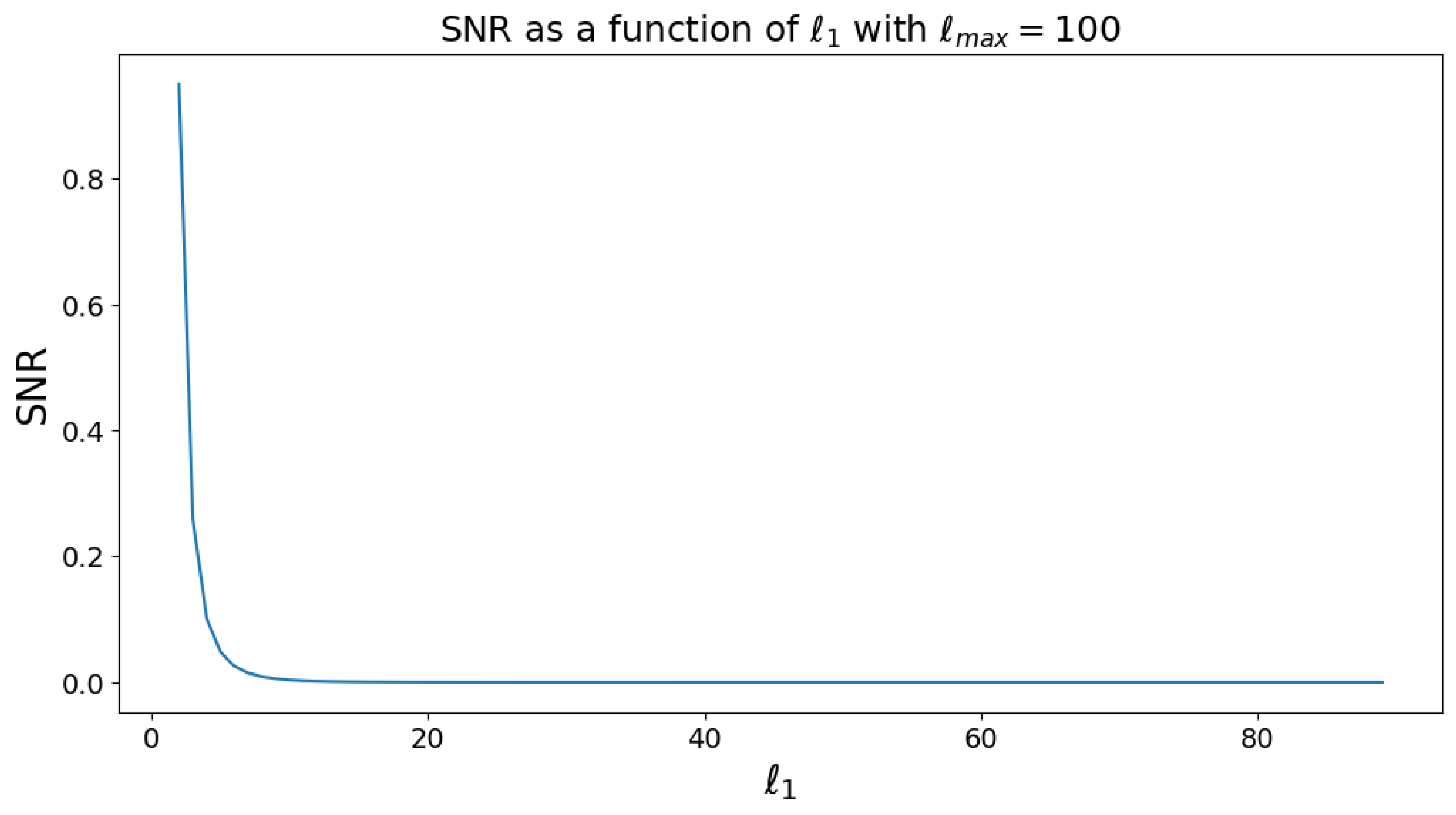

Summary

- We applied a toy model primordial curvature parity-odd trispectrum, evolved with linear growth factor and transfer functions and then projected, to obtain the weak lensing trispectrum.

- We estimated its signal-to-noise ratio, suggesting that weak lensing may provide a complementary probe of parity-odd information at late times.

Trispectrum template

- Gaussian random field primordial curvature perturbation $\xi_G(\boldsymbol{k})$:

$$\xi_G(\boldsymbol{k}) = \sqrt{\frac{V_{box}\pi^2 A_s}{k^3}\left(\frac{k}{k_p}\right)^{n_s-1}}\,[N_1(\boldsymbol{k}) + iN_2(\boldsymbol{k})]$$

N_1 and N_2 are drawn from a standard normal distribution. $k_p = 0.05\ \mathrm{Mpc}^{-1}$ is the pivot scale.

$$P_{\mathcal{R}}(k) = \frac{2\pi^2}{k^3} A_s(k_p)\left(\frac{k}{k_p}\right)^{n_s-1}$$

Transform this Gaussian random field into a non-Gaussian field:

$$\xi(\boldsymbol{x}) = \xi_G(\boldsymbol{x}) + g_-\nabla\xi_G^{[\alpha]}(\boldsymbol{x}) \cdot [\nabla\xi_G^{[\beta]}(\boldsymbol{x}) \cdot \nabla\xi_G^{[\gamma]}(\boldsymbol{x})]$$

g_- controls the amplitude of the primordial parity-odd trispectrum, and the modes of the fields in triple product are:

$$\xi_G^{[\alpha]}(k) = k^\alpha \xi_G(k)$$

The leading order imaginary part of the trispectrum for this template is:

$$T_-(\boldsymbol{k}_1, \boldsymbol{k}_2, \boldsymbol{k}_3) = g_-\boldsymbol{k}_1 \cdot (\boldsymbol{k}_2 \times \boldsymbol{k}_3)\,(2\pi^2 A_s)^3\,(k_1^{\alpha-4+n_s} k_2^{\beta-4+n_s} k_3^{\gamma-4+n_s} k_4^0 \mp 23\ \text{signed permutations})$$

Coulton et al. 2024

Weak lensing convergence angular power spectrum

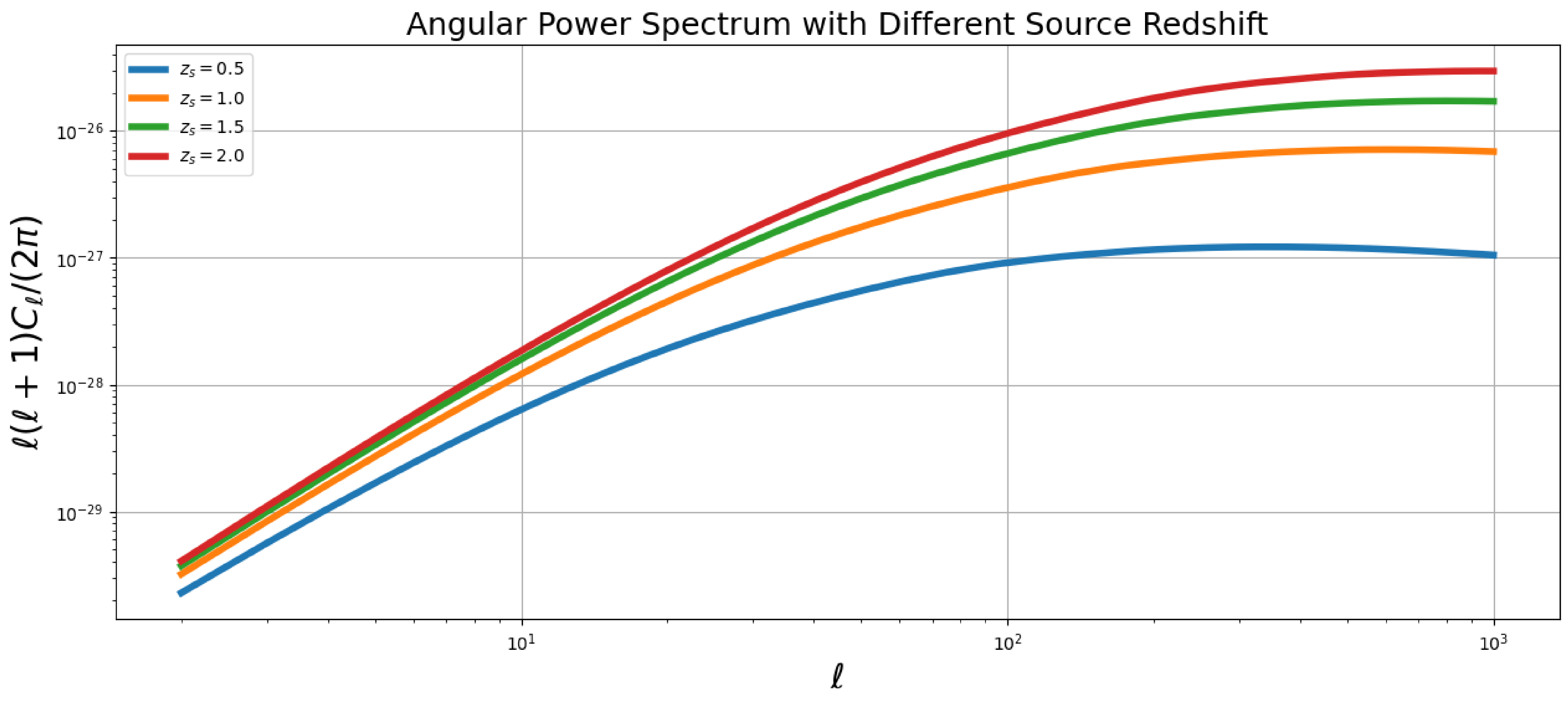

Isotropic N-point basis function

- Isotropic functions of positions $r_1, r_2, \ldots, r_N$ are invariant under simultaneous rotations of all the coordinates.

Our generalization of the addition theorem for spherical harmonics is a set of basis functions $\mathcal{P}(\mathbf{R})$, with $\mathbf{R} \equiv (\mathbf{r}_1, \mathbf{r}_2, \ldots, \mathbf{r}_N)$, invariant under simultaneous rotations $\mathcal{R}$ of all the coordinates:

$$\mathcal{P}(\mathcal{R}\mathbf{R}) = \mathcal{P}(\mathbf{R}). \qquad (2)$$

- Use spherical harmonics and Clebsch-Gordan coefficients to express them.

- If the summation of all ell's from the spherical harmonics is odd, then the basis is parity odd, otherwise parity even.

$$\mathcal{P}_{111}(\hat{\boldsymbol{r}}_1, \hat{\boldsymbol{r}}_2, \hat{\boldsymbol{r}}_3) = -\sum_{m_i} \begin{pmatrix} 1 & 1 & 1 \\ m_1 & m_2 & m_3 \end{pmatrix} Y_{1m_1}(\hat{\boldsymbol{r}}_1) Y_{1m_2}(\hat{\boldsymbol{r}}_2) Y_{1m_3}(\hat{\boldsymbol{r}}_3)$$

$$\mathcal{P}_{111}(\hat{\boldsymbol{r}}_1, \hat{\boldsymbol{r}}_2, \hat{\boldsymbol{r}}_3) = -\frac{3i}{\sqrt{2}(4\pi)^{3/2}} \hat{\boldsymbol{r}}_1 \cdot (\hat{\boldsymbol{r}}_2 \times \hat{\boldsymbol{r}}_3)$$

Why 2D surface doable?

- On 2D flat plane, a parity transformation is equivalent to a $180°$ rotation about the axis perpendicular to the plane through the origin.

$$\mathcal{R}(\theta) = \begin{pmatrix} \cos\theta & -\sin\theta \\ \sin\theta & \cos\theta \end{pmatrix}$$

$$\mathcal{R}(\pi) = \begin{pmatrix} \cos\pi & -\sin\pi \\ \sin\pi & \cos\pi \end{pmatrix} = \begin{pmatrix} -1 & 0 \\ 0 & -1 \end{pmatrix} = \mathbb{P} = \begin{pmatrix} -1 & 0 \\ 0 & -1 \end{pmatrix}$$

- But this is not true for 2D curved surface.

Why 2D surface doable?

- **Rotation on 2D spherical surface**

$$\mathcal{R}(\alpha,\beta,\gamma)=\mathcal{R}_x(\gamma)\mathcal{R}_y(\beta)\mathcal{R}_z(\alpha)$$
$$=\begin{pmatrix}\cos\gamma & -\sin\gamma & 0\\ \sin\gamma & \cos\gamma & 0\\ 0 & 0 & 1\end{pmatrix}\begin{pmatrix}\cos\beta & 0 & \sin\beta\\ 0 & 1 & 0\\ -\sin\beta & 0 & \cos\beta\end{pmatrix}\begin{pmatrix}1 & 0 & 0\\ 0 & \cos\alpha & -\sin\alpha\\ 0 & \sin\alpha & \cos\alpha\end{pmatrix}$$

- **Determinant:**

$$|\mathcal{R}(\alpha,\beta,\gamma)|=|\mathcal{R}_x(\gamma)|\,|\mathcal{R}_y(\beta)|\,|\mathcal{R}_z(\alpha)|=1$$

- **Parity transformation in 3D space**

$$\mathbb{P}=\begin{pmatrix}-1 & 0 & 0\\ 0 & -1 & 0\\ 0 & 0 & -1\end{pmatrix}$$

- **Determinant:**

$$|\mathbb{P}|=-1$$

Greco et al. 2025

Signal-to-Noise Ratio

- Separate the contributions from the unconnected or Gaussian piece and the connected r trispectrum piece

$$Q^{\ell_1\ell_2}_{\ell_3\ell_4}(L) = G^{\ell_1\ell_2}_{\ell_3\ell_4}(L) + T^{\ell_1\ell_2}_{\ell_3\ell_4}(L)$$

- Gaussian noise variance

$$\langle G^{\ell_1\ell_2 *}_{\ell_3\ell_4}(L) G^{\ell_1\ell_2}_{\ell_3\ell_4}(L') \rangle = (2L+1)\,\delta_{LL'} C^{tot}_{\ell_1} C^{tot}_{\ell_2} C^{tot}_{\ell_3} C^{tot}_{\ell_4}$$

Weak lensing trispectrum projection part

- **Projection part:**

$$\mathcal{I}^{\ell_1'\ell_2'\ell_3'}_{\ell_1\ell_2\ell_3\ell_4} = \left[\frac{2}{5}\frac{1}{\Omega_{m,0}H_0^2}\right]^4 \int_0^\infty \frac{\mathrm{d}\chi}{\chi^{14}} \times \prod_{n=1}^{4} \left[q_n(\chi) D(\chi) \mathcal{T}_\delta\left(\frac{\ell_n}{\chi}\right) \ell_n^2\right] \times T^{\mathcal{R}}_{\ell_1'\ell_2'\ell_3'}\left(\frac{\ell_1}{\chi}, \frac{\ell_2}{\chi}, \frac{\ell_3}{\chi}, \frac{\ell_4}{\chi}\right)$$

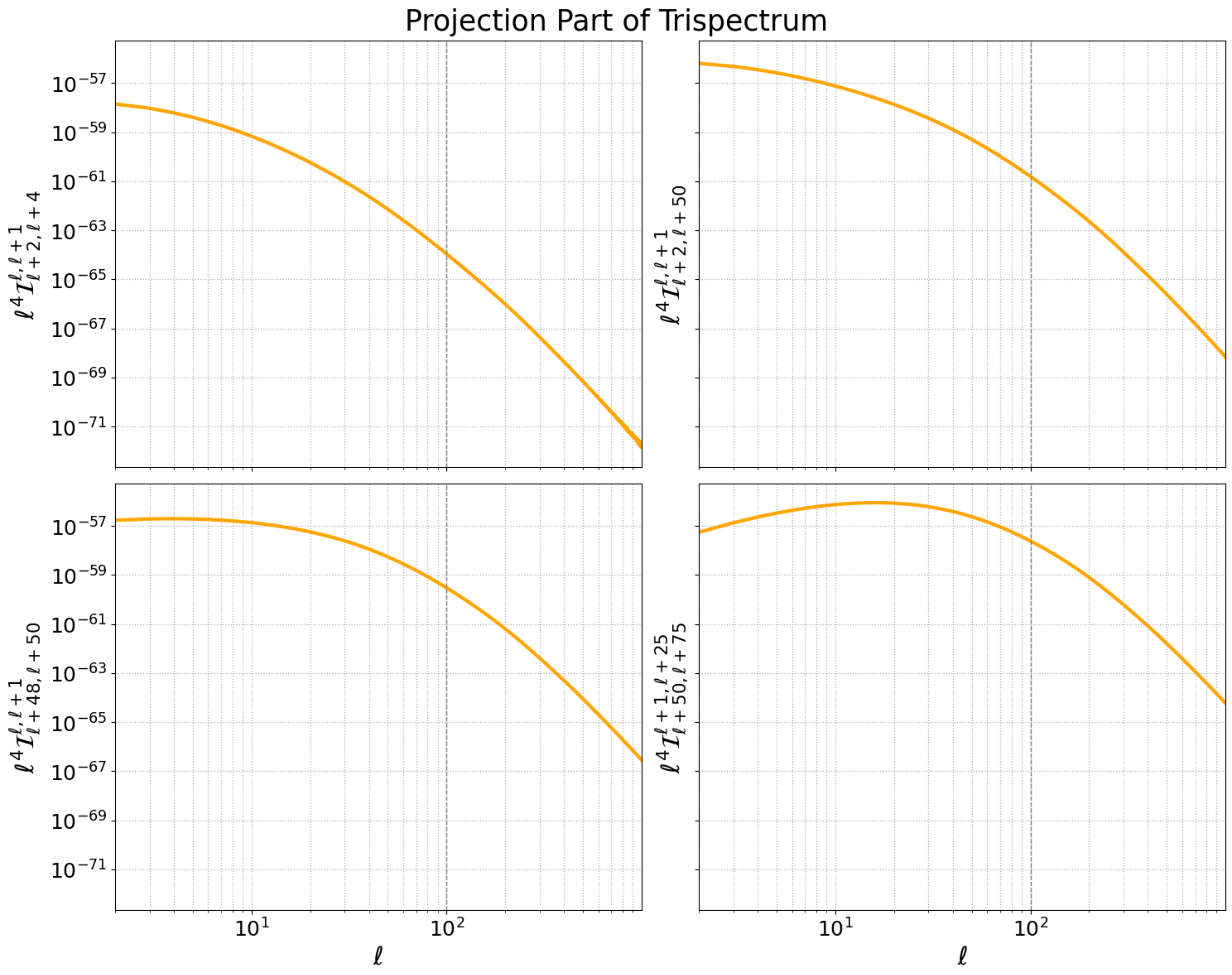

Weak lensing trispectrum projection part

- **Projection part:**

$$\mathcal{I}^{\ell_1'\ell_2'\ell_3'}_{\ell_1\ell_2\ell_3\ell_4} = \left[\frac{2}{5}\frac{1}{\Omega_{m,0}H_0^2}\right]^4 \int_0^\infty \frac{\mathrm{d}\chi}{\chi^{14}}$$
$$\times \prod_{n=1}^{4} \left[q_n(\chi) D(\chi) \mathcal{T}_\delta\left(\frac{\ell_n}{\chi}\right)\ell_n^2\right]$$
$$\times T^{\mathcal{R}}_{\ell_1'\ell_2'\ell_3'}\left(\frac{\ell_1}{\chi},\frac{\ell_2}{\chi},\frac{\ell_3}{\chi},\frac{\ell_4}{\chi}\right)$$

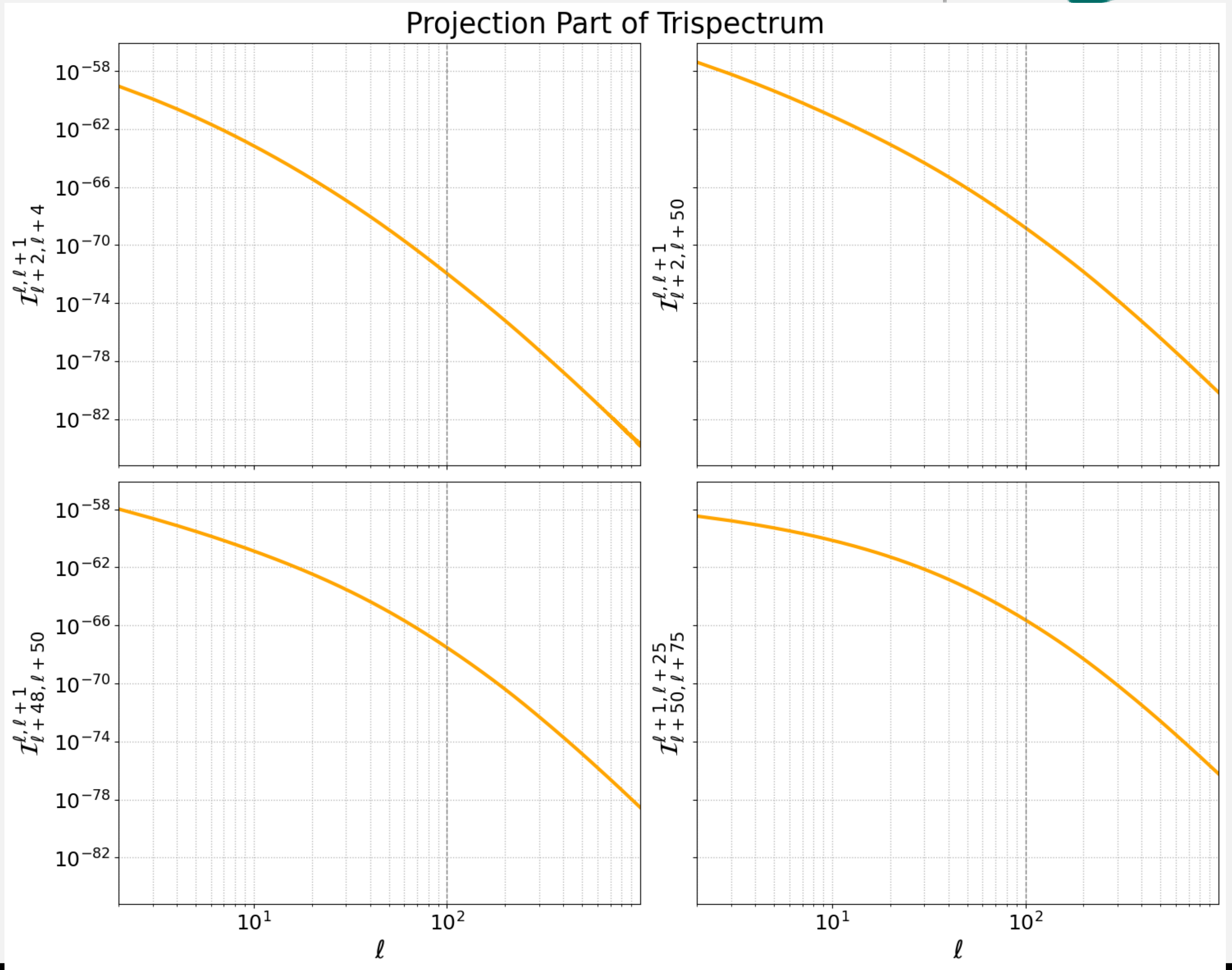

Extended Limber approximation

- **Limber approximation**

$$j_\ell(k\chi) \propto \delta_D^{[1]}\left(k - \frac{\ell}{\chi}\right)$$

- **Higher orders:**

$$\int \mathrm{d}r\, f(r) J_\nu(kr) = \frac{1}{k}\left[f\left(\frac{\nu}{k}\right) - \frac{1}{2k^2} f''\left(\frac{\nu}{k}\right) - \frac{\nu}{6k^3} f'''\left(\frac{\nu}{k}\right) + \dots\right]$$

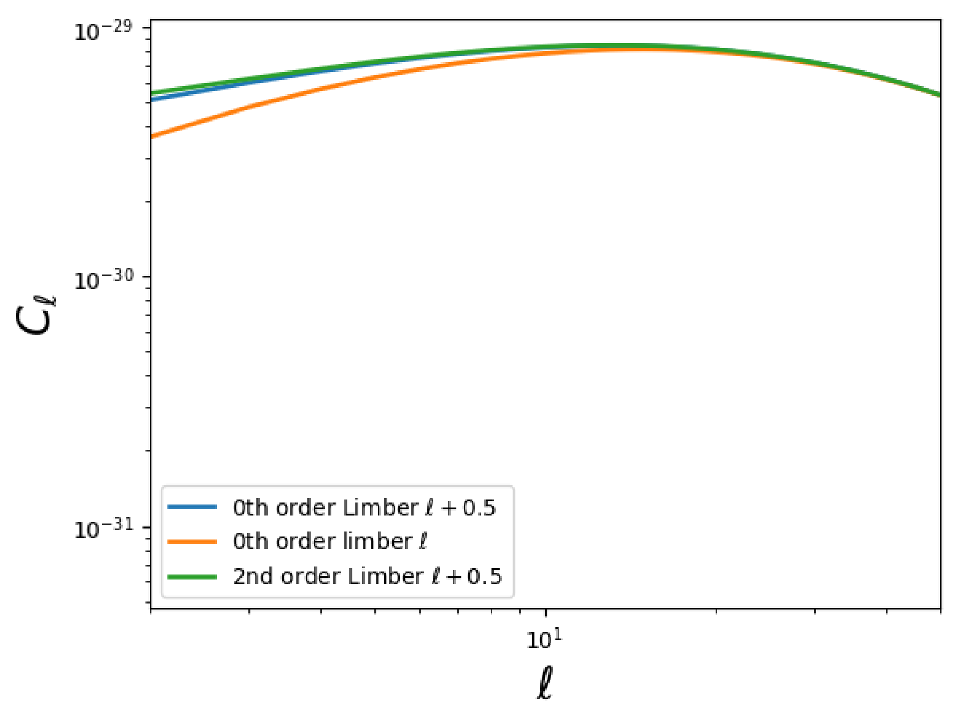

LoVerde et al. 2008

Geometry part